Motion of water and sediment due to non-breaking waves in the swash zone*

Jarosław Kapiński*
Rafał Ostrowski

Institute of Hydro-Engineering,
Polish Academy of Sciences
(IBW PAN),
Kościerska 7, Gdańsk 80–328, Poland;

e-mail: kapinski@ibwpan.gda.pl

*corresponding author

Abstract

A long wave run-up theory is applied to the modelling of wave-induced flow velocities, sediment transport rates and bottom changes in a swash zone. First, the properties of the water tongue motion and the resulting lithodynamic response are analysed theoretically. Next, an attempt is made to run the model for the natural conditions encountered on the southern Baltic Sea coast. The Lagrangian swash velocities are used to determine the Eulerian phase-resolved bed shear stresses with a momentum integral method, after which the motion of sand is described by the use of a two-layer model, comprising bedload and nearbed suspended load. Seabed evolution is then found from the spatial variability of the net sediment transport

The complete text of the paper is available at http://www.iopan.gda.pl/oceanologia/

rates. The results presented are limited to cases of the small-amplitude waves that seem to be responsible for accretion on beaches.

1. Introduction

The evolution of sandy sea shores usually involves a huge part of the cross-shore transect, from an offshore location called the 'depth of closure', through the system of nearshore bed forms (e.g. bars), to the shoreline and the exposed part of the beach. This complex process has long fascinated coastal researchers and engineers and has been the subject of numerous theoretical and experimental investigations. For instance, a very thorough analysis of the capability of cross-shore profile models was presented by Van Rijn et al. (2003). That study was based on a comparison of theoretical results with 2D large scale laboratory data and a field experiment performed during the EU-COAST3D project. Although considerable progress was made in the modelling, some shortcomings and inaccuracies of the contemporary models were pointed out. In particular, these problems concern areas of very shallow water close to the shoreline, especially the swash zone, where the sea-land interface moves continuously. Difficulties in modelling hydrodynamic and lithodynamic processes near the shoreline were also encountered, e.g. by Ostrowski (2003), while modelling the evolution of a multi-bar cross-shore profile.

The location of the swash zone, which separates the emerged part of the cross-shore profile from its submerged part, depends mainly on the position of the mean water level. It should be noted, however, that even in non-tidal seas the emerged part of the beach is occasionally flooded, especially during storm surges. On the southern Baltic coast, storm surges typically rise to 1 m, and sometimes almost 2 m, above the mean still water level.

Bearing in mind the accelerating rise in the Baltic Sea level (see e.g. Pruszak & Zawadzka 2005), as well as the forecast increase in the frequency of severe storms due to climate change, one should expect the occurrence of high sea water levels to become more common. In such circumstances, the swash zone will move landwards and wave run-up may affect the dune toe, as shown in Figure 1.

In view of the above, it seems worthwhile seeking a reliable method of predicting hydrodynamic and lithodynamic processes in the swash zone of natural sandy beaches; in particular, one capable of modelling sediment transport rates and the evolution of this part of the sea shore would be highly desirable.

The present study follows a conventional approach, within which seabed evolution is assumed to be taking place as a result of the spatial variability of net sediment transport rates. These rates along the cross-shore profile
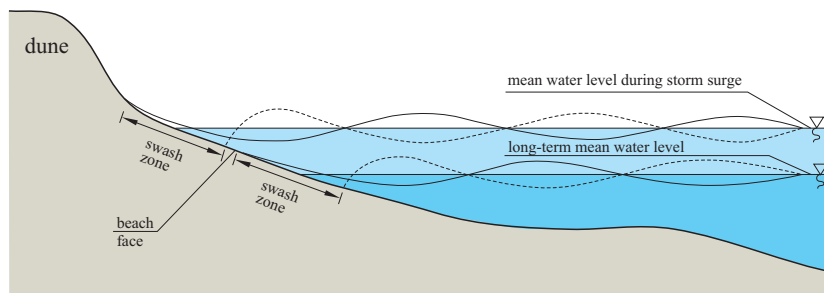
Figure 1. Migration of the swash zone during a storm surge

depend on the instantaneous rates at each individual location during the wave period. As mentioned before, determining the instantaneous hydrodynamic and lithodynamic parameters in the region of a moveable boundary of an aquatic environment is problematic. To date, there have been a few attempts to solve this problem, and a number of more or less sophisticated theoretical and experimental approaches have been proposed and reviewed (see e.g. Butt & Russell 2000, Kobayashi & Johnson 2001, Larson et al. 2001, Alsina et al. 2005, Masselink & Puleo 2006). These studies, however, deal mostly with waves breaking on the beach face.

Nevertheless, the available studies do provide many interesting and insightful findings. For instance, Nielsen (2002) showed that the flow velocity during a rapidly accelerating up-rush generates much stronger bed shear stresses (and sediment transport rates) than the same velocity during a mildly accelerating down-rush flow. Further, this author points to a number of physical processes that complicate the problem, e.g. the lag between instantaneous bed shear stresses and instantaneous sediment transport rates, pre-suspension of sediment from bore collapse versus very high concentrations in the sheet flow layer, as well as infiltration and fluidization. The study by Pritchard & Hogg (2005) triggers similar doubts and queries, especially concerning the qualitative and quantitative imbalance between onshore and offshore transport, dependent as this is on contributions from sediment entrained within the swash zone and that from sediment suspended by the initial bore collapse. The discussion of this issue is continued by Baldock & Alsina (2005), who anticipated distinct difficulties in further theoretical and experimental investigations into the hydro-, litho- and morphodynamics of the swash zone.

Although considerable progress in swash zone modelling has been made and some models simulating time-dependent sediment transport rates have been derived for the swash zone, it appears that knowledge of the swash zone

is still far from complete: a wholly reliable, detailed description of swash zone lithodynamics has yet to be achieved. Therefore, any new proposals in this respect will be attractive only if they fill a gap in our existing knowledge of swash zone behaviour.

Migration of the shoreline is caused by the incessant process during which sandy beaches are subject to erosion or accretion. The latter is less spectacular but equally important in reshaping coastal bathymetry. It is thought that accretionary conditions prevail during periods dominated by long, non-breaking waves. This case is considered in the paper, which follows the classical deterministic approach, comprising a theoretical description of the physical processes occurring in coastal zones. Within this modelling system, wave transformation in shallow water, including the swash zone, is determined first; this is done using the Lagrangian approach. Then the bed shear stresses are calculated, from which the sediment transport rates are found. The proposed approach displays a highly nonlinear relationship between the swash velocity and the bed shear stress (the stress depends on both the velocity and the acceleration). This property was identified and described, e.g. by Nielsen (2002).

The velocities, bed shear stresses and sediment transport rates are determined in phase-resolving mode, yielding instantaneous values for the entire wave period. From an integration of the sediment transport rates over the wave period in the individual locations of the swash zone, the net transport rates are obtained.

2. Theoretical background

2.1. Shallow water and swash zone hydrodynamics

There are a large number of phase-resolving models that predict water wave transformation in coastal areas. Many of them include complex, non-linear phenomena occurring from a limited depth to the shore. However, they are usually incapable of making computations for the beach face. This arises from the difficulty of producing an exact mathematical description of a continuously migrating shoreline – this is known as the moving boundary problem. Finally, the upshot of this shortcoming is that the mechanisms driving sediment transport at the sea-land interface are insufficiently understood. If we are to include the swash zone in the computational domain of the traditional shallow-water wave theory, which is elaborated in the Eulerian manner, we have to apply additional, more or less accurate treatments. The different techniques that can be utilized here are reviewed by e.g. Kobayashi (1999) and Prasad & Svendsen (2003).

In recent years, shallow-water wave models have been developed that have successfully applied the Lagrangian frame of reference. In this approach, there are usually no problems with the moving boundary at the landward end and so the motion of a water tongue on a beach face can be predicted exactly, including instantaneous water elevations and flow velocities. This property was confirmed by several models (see e.g. Shuto 1967, Zelt & Raichlen 1990, Kapiński 2003). The various advantages of applying the Lagrangian method to the modelling of shallow-water wave motion were briefly reviewed by Kapiński (2006).
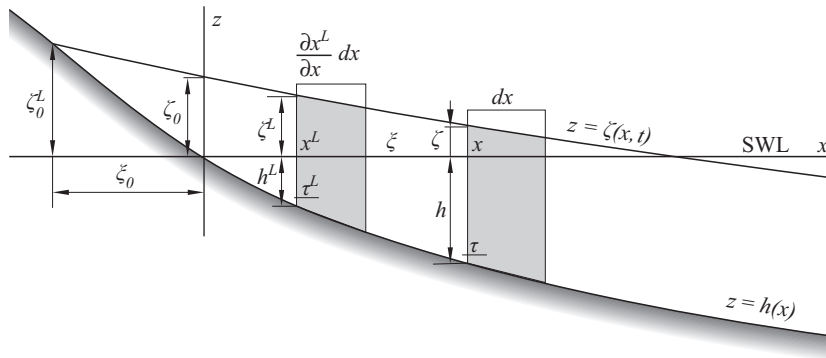
Figure 2. Definition sketch of the wave run-up model

In the present paper, the shallow-water wave model (Kapiński 2003), with some further improvements, is applied to the prediction of water motion in the swash zone. A definition sketch of the model is shown in Figure 2, where the separate parameters can be written as follows:

$$
\begin{aligned}
\xi &= \xi(x,\,t), & x^L &= x^L(x,\,t) = x + \xi(x,\,t), & \xi_0 &= \xi(x = 0,\,t), \\
\zeta &= \zeta(x,\,t), & \zeta^L &= \zeta^L(x^L,\,t) = \zeta^L(x + \xi,\,t), & \zeta_0 &= \zeta(x = 0,\,t), \\
h &= h(x), & h^L &= h^L(x^L) = h^L(x + \xi), & \zeta_0^L &= \zeta^L(x^L = \xi,\,t).
\end{aligned}
\tag{1}
$$

The theory is based on the laws of momentum and mass conservation, which are expressed in the Lagrangian description:

$$
\rho V^L a^L + V^L \nabla p^L = F^L \qquad \text{and} \qquad \rho V = \rho V^L,
\tag{2}
$$

where
a^L – acceleration of a water parcel,
p^L – vertical distribution of water pressure at x^L,
ρ – water density,
F^L – sum of all external forces acting on the parcel,

V, V^L – volume of the parcel at initial position x and at instantaneous position x^L, respectively.

The parameters used in equation (2), taking into account the notation from Figure 2, are given by (per unit width if applicable):

$$a^L = \frac{\partial^2 \xi}{\partial t^2}, \qquad p^L = p_0 + \rho g \left(\zeta^L - z \right), \tag{3}$$

$$V = h dx, \qquad V^L = \left(h^L + \zeta^L \right) dx^L, \tag{4}$$

$$F^L = \tau^L dx^L, \tag{5}$$

where

$$dx^L = \frac{\partial x^L}{\partial x} dx.$$

The dissipative term F^L includes the bottom friction. It has been dropped here, so that $F^L = 0$, because the friction will be taken into consideration in the sediment transport module.

After simplifying assumptions concerning the small-amplitude wave motion and gentle bottom changes, the governing set of equations driving the orbital motion takes the following form:

$$\frac{\partial^2 \xi}{\partial t^2} + g \frac{\partial \zeta^L}{\partial x} = 0, \qquad \frac{\partial^2 \zeta^L}{\partial t^2} - \frac{\partial}{\partial x} \left(gh \frac{\partial \zeta^L}{\partial x} \right) = 0, \tag{6}$$

where ξ and ζ^L denote the depth-averaged horizontal and vertical water-surface particle displacements respectively, g is the acceleration due to gravity and h is the still water depth.

In an earlier paper (Kapiński & Kołodko 1996) the governing equations were derived for simplified conditions in which the bathymetry consists of two parts: (a) a shallow water area with a constant bottom depth, and (b) a beach slope with a constant inclination. This leads to the following equation:

$$R/H = \left| J_0 \left(\sqrt{\beta_r l} \right) + i J_1 \left(\sqrt{\beta_r l} \right) \right|^{-1} = \left(J_0^2 \left(\sqrt{\beta_r l} \right) + J_1^2 \left(\sqrt{\beta_r l} \right) \right)^{-0.5}, \tag{7}$$

where
R/H – relative wave run-up height,
J_0, J_1 – Bessel functions of the first and second order, respectively. Equation (7) is the analytical solution for small-amplitude standing waves on a uniform slope; it is known as the Keller & Keller (1964) formula.

In the hydrodynamic model the linear shallow-water wave theory has been adopted and applied to describe the wave motion on a beach face. So,

the limitations of the validity concerning the swash zone are the same as for the theory extended to this area.

Shuto (1967) observed that the generated wave train in the Lagrangian description differs slightly from the sinusoidal profile. This seemingly minor discrepancy significantly changes the water flow pattern (Kapiński 2006). Therefore, a transfer function of the free water elevation at the seaward boundary was derived and applied here. As a consequence, both modelled initial wave profiles and the water motion are described by the first harmonics as realized in the traditional Eulerian description. Such advantages of the Lagrangian wave approach, like direct simulation of orbital motion and tracking the motion of a moving shoreline, have been retained here.

The forecasting of the cross-shore profile change of a beach face is based on the flow velocity field. The computational domain comprises the permanently submerged part of the beach slope as well as the part that is alternately wet and dry. First, time-dependent orbital velocities $\partial\xi/\partial t$ are transformed to flow velocities U. This is carried out for selected locations on the beach slope, from the slope toe to the wave run-up limit. Next, these velocities are used to compute magnitudes of the friction velocity u_f, which is the direct driving force for sediment motion. Thus, the Lagrangian displacements ξ are indirectly used in section 2.2 to predict the Eulerian sediment transport rates and bottom profile changes at fixed points on the beach face.

2.2. Bed shear stresses, sediment transport and bottom changes

According to the assumptions of the present theoretical model, the motion of sediment is caused by the bed shear stress ($\tau = \rho u_f{}^2$) induced by the oscillatory motion of water on the beach face. The instantaneous values of the friction velocity u_f during a wave period are determined by the momentum integral method for wave-current flow proposed by Fredsøe (1984). For the case of pure oscillatory motion, Fredsøe (1984), using the dimensionless variable z_1 described as

$$z_1 = \frac{U\kappa}{u_f} \tag{8}$$

derived the following differential equation:

$$\frac{dz_1}{d(\omega t)} = \frac{30\kappa^2 U}{k_e \omega e^{z_1}(z_1 - 1) + 1} - \frac{z_1(e^{z_1} - z_1 - 1)}{e^{z_1}(z_1 - 1) + 1} \; \frac{1}{U} \; \frac{dU}{d(\omega t)}. \tag{9}$$

The input data of the above equation consist of the von Karman constant $\kappa = 0.4$, the angular frequency ω of the wave motion, the free stream velocity

$U(\omega t)$ and the bed roughness height k_e. From the solution of equation (9), the function $z_1(\omega t)$ is obtained, on the basis of which one can calculate the time-dependent friction velocity $u_f(\omega t)$ from equation (8), as well as the distribution of the boundary layer thickness $\delta(\omega t)$ over the wave period, using the following formula:

$$\delta = \frac{k_e}{30}\left(e^{z_1} - 1\right).\tag{10}$$

It should be noted that, in view of equations (8) and (9), the bed shear stress ($\tau = \rho u_f{}^2$) depends on both the free-stream velocity U and the flow acceleration $dU/d(\omega t)$, which is in agreement with the concept of Nielsen (2002).

The shear stresses are the driving force of sediment transport rates, which are determined using the model of Kaczmarek & Ostrowski (2002). Successful, thorough testing versus experimental data allows this model to be adapted and applied within the computational framework presented here. The sediment transport model comprises the bedload layer (below the theoretical bed level) and the layer of nearbed suspension, named the contact load layer in the study by Kaczmarek & Ostrowski (2002). This two-layer sediment transport model is briefly presented below.

The mathematical model of bedload transport is based on the water-soil mixture approach, with a collision-dominated drag concept and the effective roughness height k_e (necessary for the determination of the bed shear stresses). The collision-dominated bedload layer granular-fluid region stretches below the theoretical bed level while the turbulent fluid region extends above it, constituting the contact load layer. The granular-fluid region below the bed is characterized by very high concentrations, where inter-granular resistance is predominant. The sediment transport modelling system applied in the present study had been previously thoroughly tested against available large scale experimental data. Some of these data were collected in pure wave conditions, but most of them in wave-current conditions where wave motion was predominant. A detailed description of the model and the results of its validation are given in Kaczmarek & Ostrowski (2002).

For known bed shear stresses $\rho u_f{}^2(\omega t)$, the instantaneous bedload velocities $u(z', t)$ and concentrations $c(z', t)$ are found from the following equations (with the vertical axis z' directed downwards from the theoretical bed level):

$$\alpha^0 \left(\frac{c - c_0}{c_m - c}\right)\sin\varphi\sin 2\psi + \mu_1 \left(\frac{\partial u}{\partial z'}\right)^2 = \rho u_f{}^2,\tag{11}$$

$$\alpha^0 \left(\frac{c - c_0}{c_m - c} \right) (1 - \sin\varphi \sin 2\psi) + (\mu_0 + \mu_2) \left(\frac{\partial u}{\partial z'} \right)^2 =$$

$$= \left(\frac{\mu_0 + \mu_2}{\mu_1} \right) \Bigg|_{c = c_0} \rho u_f{}^2 + (\rho_s - \rho)g \int\limits_0^{z'} c\,dz' \tag{12}$$

in which

ρ_s – soil density,

α^0 – a constant,

c_0 – sediment concentration corresponding to soil fluidity,

c_m – sediment concentration corresponding the closest possible packing of grains,

μ_0, μ_1 and μ_2 – functions of the solid concentration c:

$$\frac{\mu_1}{\rho_s d^2} = \frac{0.03}{(c_m - c)^{1.5}}\,, \qquad \frac{\mu_0 + \mu_2}{\rho_s d^2} = \frac{0.02}{(c_m - c)^{1.75}}\,, \tag{13}$$

where d – grain diameter of the seabed soil.

The value φ in equations (11) and (12) is the quasi-static angle of internal friction, while the angle ψ between the major principal stress and the horizontal axis (for simple shear flow) is equal to

$$\psi = \frac{\pi}{4} - \frac{\varphi}{2}\,. \tag{14}$$

In the calculations the following values are assumed:

$$\frac{\alpha^0}{\rho_s g d} = 1\,, \qquad c_m = 0.53\,, \qquad c_0 = 0.32\,, \qquad \varphi = 24.4^\circ\,. \tag{15}$$

All of the parameters and constants used in the bedload model have remained unchanged since the model was tested by Kaczmarek & Ostrowski (2002).

In the contact load layer, following Deigaard (1993), the sediment velocity and concentration are modelled using the equations below (with the vertical axis z directed upwards from the theoretical bed level):

$$\left[\frac{3}{2} \left(\alpha \frac{d}{w_s} \frac{du}{dz} \frac{2}{3} \frac{s + c_M}{c_D} + \beta \right)^2 d^2 c^2 (s + c_M) + l^2 \right] \left(\frac{du}{dz} \right)^2 = u_f'^2\,, \tag{16}$$

$$\left[3 \left(\alpha \frac{d}{w_s} \frac{du}{dz} \frac{2}{3} \frac{s + c_M}{c_D} + \beta \right)^2 d^2 \frac{du}{dz} c + l^2 \frac{du}{dz} \right] \frac{dc}{dz} = -w_s c\,. \tag{17}$$

The term $u_f'^2(\omega t)$ is related to the 'skin friction', calculated by Fredsøe's (1984) model for the 'skin' roughness $k_e' = 2.5d$. In equations (16) and

(17) w_s denotes the settling velocity of grains, s stands for the relative soil density (ρ_s/ρ), c_M and c_D are the added mass and drag coefficients, respectively, α and β are the coefficients introduced by Deigaard (1993), and l is the mixing length defined as $l = \kappa z$ (where κ is the von Karman constant).

Assuming that the sediment velocity distribution in the contact load layer is logarithmic at a certain distance from the bed and that the roughness related to this profile depends on the coefficient α, an iterative procedure was proposed by Kaczmarek & Ostrowski (1998) to find this coefficient. It is further assumed that the coefficients α and β in the contact load model are equal. Parameters c_D and c_M were selected during the testing of the model; they have remained unchanged since the publication of Kaczmarek & Ostrowski (2002). Their values, together with some other important constants, are given in Table 1.

Table 1. Values of the parameters used in the contact load model

c_M	c_D	ρ_s [kg m^{-3}]	κ	$d = d_{50}$ [mm]
0.35	1.0	2650	0.4	0.22

The instantaneous sediment transport rates are computed from distributions of velocity and concentration in the bedload layer and in the contact load layer:

$$q_{b+c}(t) = \int_0^{\delta_b} u(z', t)\, c(z', t)dz' + \int_{k_e'/30}^{\delta_c} u(z, t)\, c(z, t)dz\,, \qquad (18)$$

where $\delta_b(\omega t)$ is the bedload layer thickness and δ_c denotes the upper limit of the nearbed suspension (contact load layer thickness). The quantity δ_b results from the solution of equations (11) and (12), while the value of δ_c is the characteristic boundary layer thickness calculated on the basis of Fredsøe's (1984) approach (see Kaczmarek & Ostrowski 2002).

The net transport rate in the bedload and contact load layers is calculated as follows:

$$q_b + q_c = \frac{1}{T}\int_0^T q_{b+c}(t)dt\,. \qquad (19)$$

In the original model, Kaczmarek & Ostrowski (2002) also included a third layer of sediment transport, named the outer region, consisting of sediment suspended in the water column high above the seabed and the

sediment motion in this layer due to a steady current, e.g. wave-induced undertow. In the case of the swash zone, however, the limited water depth allows one to concentrate on the nearbed layers in which sediment transport is the most intensive.

The net sediment transport rates are calculated along the shallow water cross-shore profile, including the swash zone. Consequently, the evolution of the nearshore seabed profile can be modelled from these net transport quantities.

Following the conventional approach, the evolution of the seabed profile is determined on the basis of the spatial variability of net sediment transport rates from the following continuity equation for sediment perpendicular to the shore direction:

$$\frac{\partial h(x,\,t)}{\partial t} = \frac{1}{1-n}\frac{\partial q(x,\,t)}{\partial x}\,, \tag{20}$$

where q denotes the total (bedload q_b and contact load q_c) net sediment transport rate $[\mathrm{m}^2\ \mathrm{s}^{-1}]$ in the cross-shore direction per unit width, n is the porosity of the seabed soil, and x and t stand for cross-shore coordinate and time respectively.

3. Features of the theoretical model

Wave run-up on an inclined beach face is a complex phenomenon, unlike the standing wave motion on a vertical wall, which seems to be a trivial problem. An example result of numerical simulations is presented in Figure 3, and the swash zone is shown in close-up in Figure 4. In these figures, the solid lines indicate selected wave profiles for the uprush phase, while the dashed lines denote the water elevations during the downrush phase.

The simulations were carried out for an incident progressive sinusoidal wave train of period $T = 8$ s and height $H = 0.1$ m. The beach slope has an inclination of 1:10 with the toe located at the depth of 0.8 m. The computed maximum run-up and run-down heights of the standing waves are $R_{\mathrm{up}} = 0.246$ m and $R_{\mathrm{down}} = -0.260$ m respectively. The behaviour of the water levels in the wave run-up and run-down phases shown in Figure 4 is distinctly more complicated than in the case of the wave run-up against a vertical wall. The corresponding positive and negative water elevations are not symmetrical in any cross-section of the swash zone; they also have different characteristics along the beach slope.

Thorough analysis of the computational results shows that three specific regions can be distinguished on the beach face. The first one extends between the maximum run-up and the junction of the still water level (SWL)
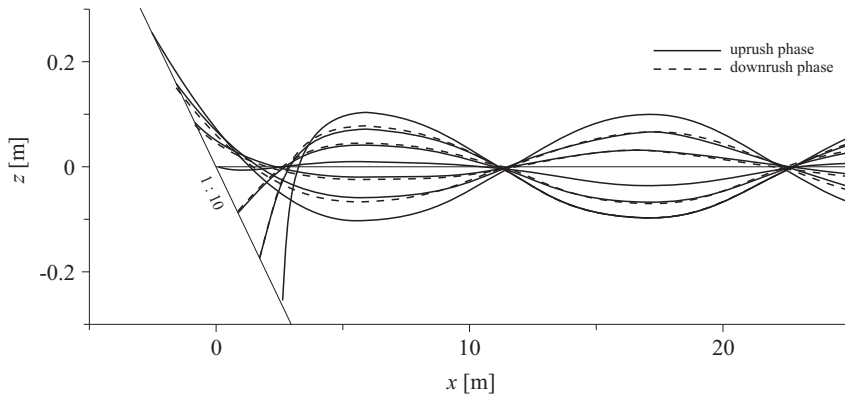
Figure 3. Standing wave motion caused by an inclined beach slope
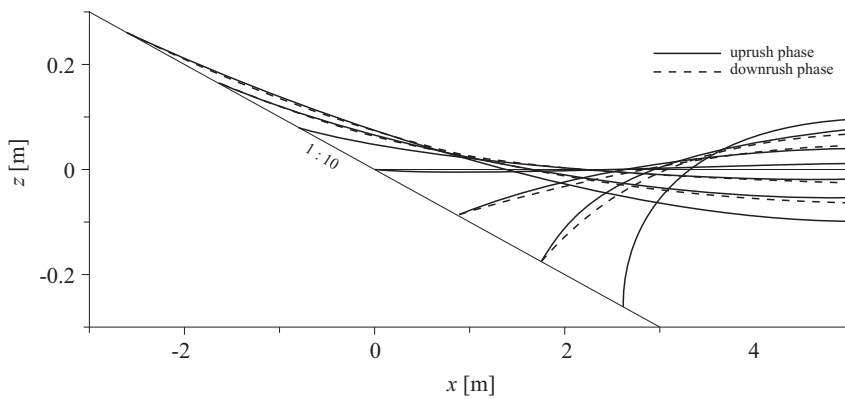
Figure 4. Water tongue transformation in the swash zone

with the beach slope. The second region is delimited by the maximum wave run-down, while the third one comprises the permanently submerged area of the beach slope. Figure 5 shows some plots of computed free water surface elevations, typical of these regions. The characteristic double humps in the middle plot are the effect of the higher harmonics of the reflected waves being superimposed on the incoming ones (these higher components appear as the effect of wave transformation over the inclined slope).

As far as the water flow velocity is concerned, two areas on the beach slope are distinguished: the swash zone and the permanently submerged area. Plots of the characteristic velocities are presented in Figure 6: here, positive magnitudes indicate the onshore direction.

The computed friction velocities u_f, which correspond to the flow velocities given in Figure 6, are presented in Figure 7. In addition, the causative velocities U from Figure 6 have been pasted onto Figure 7.
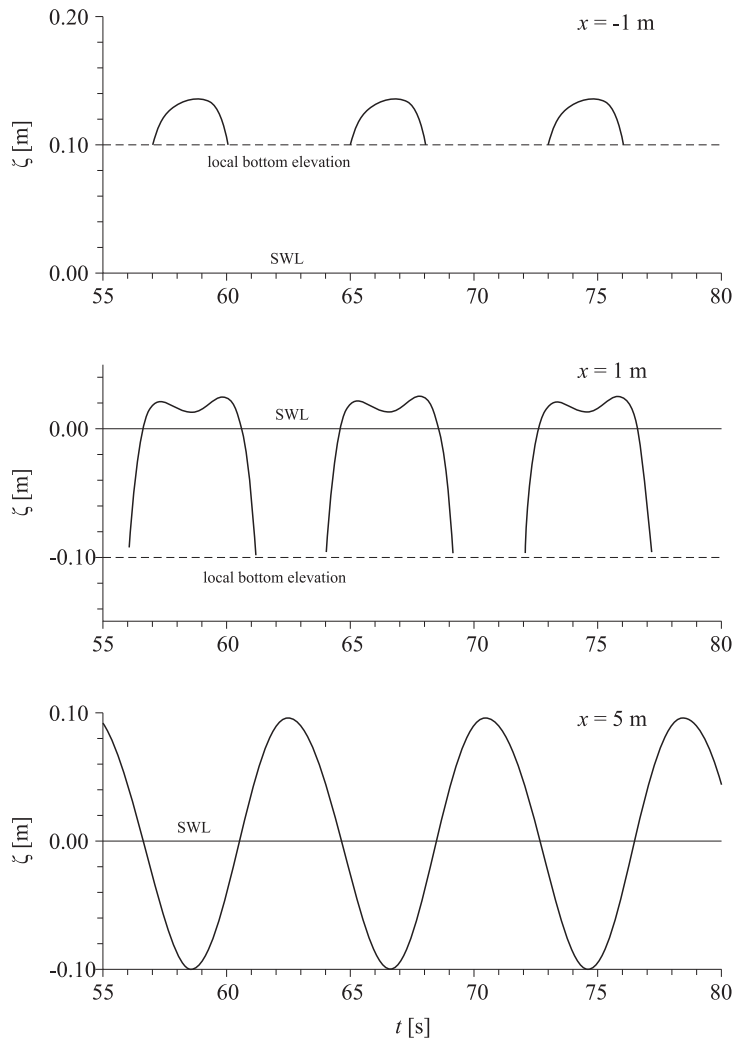
Figure 5. Water elevations characteristic of the run-up area ($x = -1$ m), run-down area ($x = 1$ m) and underwater part of the slope ($x = 5.0$ m)

According to the integral momentum model proposed by Fredsøe (1984), the bed boundary layer 'develops' during the phase of the wave crest and the boundary thickness increases to infinity (at $\omega t = \pi$). When the flow reverses (the wave trough starts), the boundary layer 'develops' again and its thickness again grows from zero to infinity (at $\omega t = 2\pi$). In the present study, only the mean boundary layer thickness (at $\omega t = \pi/2$) was used, while the friction velocity u_f was calculated as a time-variable quantity. Because of these features of the Fredsøe (1984) model, this function (although continuous) is not smooth at $\omega t = \pi$.
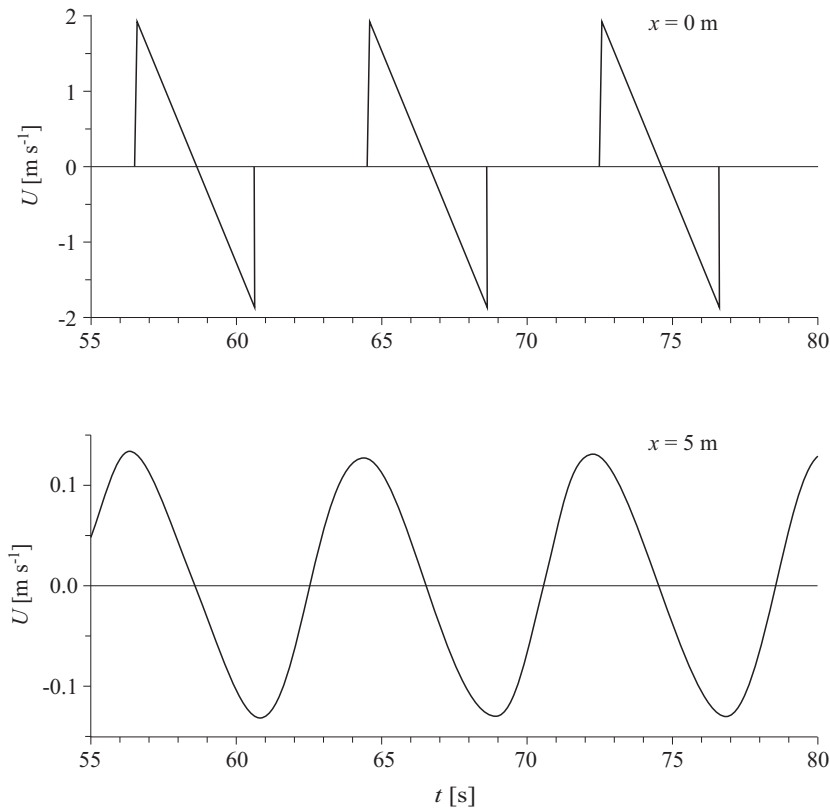
Figure 6. Flow velocities characteristic of the swash zone ($x = 0$ m) and the submerged area ($x = 5$ m)

Next, sediment transport rates were computed for the same wave ($H = 0.1$ m, $T = 8$ s) running up a plane slope. The grain size diameter was assumed to be $d = 0.22$ mm (a typical value for southern Baltic sandy beaches), with the settling velocity $w_s = 0.028$ m s^{-1}. The results presented in Figure 8 show the rates of bedload (q_b), suspended load (q_s) and total load (q_{total}). The effect of simulating bottom changes for 24 hours is shown in Figure 9.

The results indicate a tendency for the sediment from the run-down area to be carried landwards to the run-up area. Therefore, the beach face experiences local accumulation in the upper part and erosion below the mean water level. A small but noticeable mound can be observed at the wave run-down limit as well. As a consequence, the beach slope in the swash zone becomes steeper under the action of standing waves. The net sediment transport patterns (Figure 8) are due to the asymmetry of the wave-induced velocities. The relation between the hydrodynamic input and
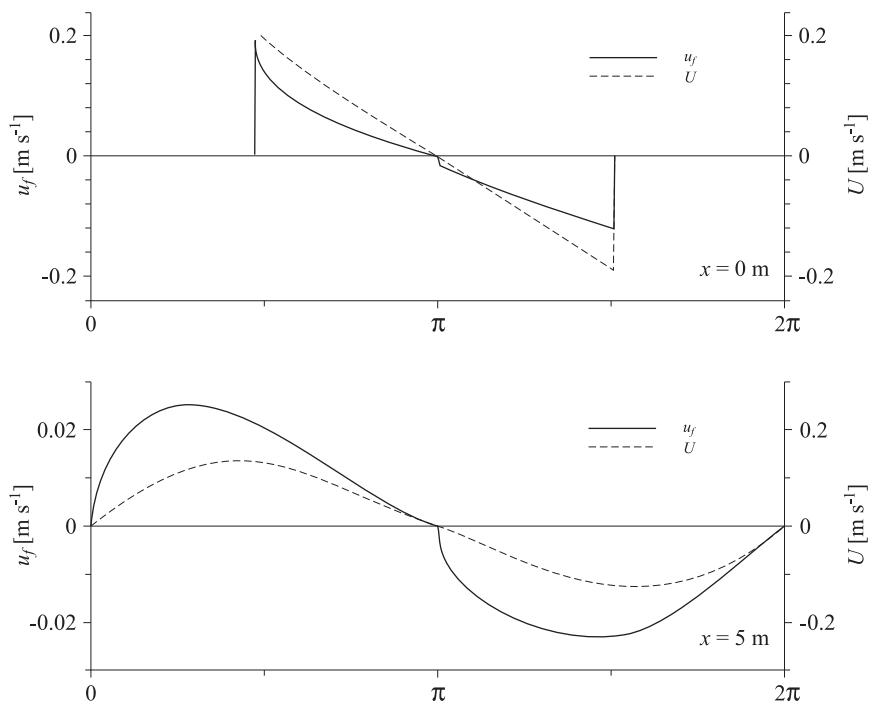
Figure 7. Friction velocity $u_f(\omega t)$ calculated for two locations on the beach face
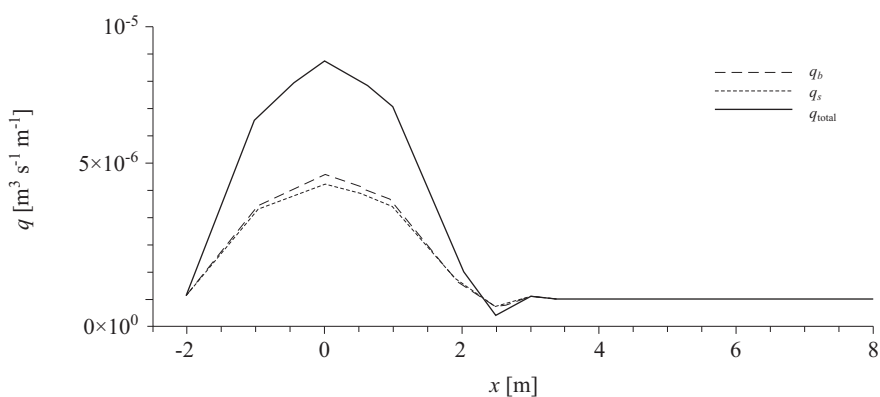
Figure 8. Computed sediment transport rates across the beach face

the bed shear stress is highly nonlinear. In the sediment transport model, the bed shear stress is the driving force for sand motion. Therefore, even a small asymmetry in nearbed velocities causes an intensive net transport in the direction of this asymmetry.

Pritchard & Hogg (2003) obtained similar results from the numerical modelling of the sediment transport rate distribution. They investigated
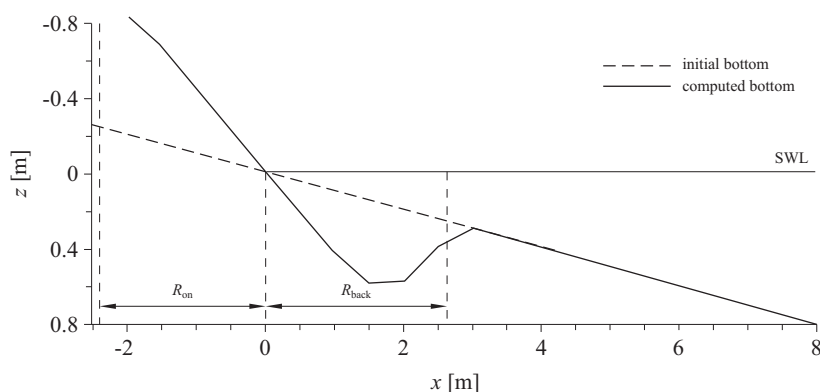
Figure 9. Computed bottom changes across the beach face

standing long waves on gently sloping muddy beaches. However, they only analysed the cross-shore transport of a fine sediment in suspension on a plane beach face, i.e. they neglected bedload transport in their modelling.

4. Field survey versus model results

The hydrodynamic model presented here yields correct results for waves of relatively small steepness. Furthermore, the slope of the swashed part of the bottom should not be too gentle, otherwise the waves would break, and wave breakage is not accounted for in the model. The example presented in the previous section lies safely within the range of the model's applicability.

It should be pointed out, however, that in the natural stormy or moderate conditions of the Baltic's dissipative, gently inclined nearshore zone, in the very shallow water near the shoreline, the wave parameters are distinctly modified as a result of earlier transformation (including breaking). During this transformation the representative wave height decreases considerably, whereas the representative period remains almost unchanged. This effect results in the appearance of not very high, long-period incident waves in front of the swash zone. In view of the above, the data set was selected from available field investigations to match the model's range of applicability.

The data were collected in 2006 on the non-tidal shore of the southern Baltic Sea, at the IBW PAN Coastal Research Station (CRS) at Lubiatowo (Poland). Among many other activities (e.g. registration of deep-water waves using a wave buoy or nearshore wave-current measurements), this field experiment surveyed wave run-up onto the beach face.

During the survey (in October and November 2006), bathymetric and tachymetric surveys were carried out a few times on the cross-shore profile. The shore at Lubiatowo slopes gently, with a large-scale mean inclination

of 1–2% (from the shoreline to about 10 m depth). The nearshore part of the cross-shore profile and the emerged beach is much steeper, reaching 5% and locally up to 10% and more.

It should be noted again that waves reach this shore having been transformed in various ways, including shoaling, multiple breaking, diffraction and refraction. Observations of the latter two effects at the site have revealed an almost perpendicular wave approach to the shoreline, regardless of deep-water wave directions. This feature, probably resulting from the gentle mean slope of the entire cross-shore profile, enabled modellers to assume that the input shallow water wave ray was perpendicular to the shoreline.

The model was run for the actual nearshore bathymetric cross-shore profile measured at CRS Lubiatowo. The seaward boundary of the profile was assumed to be ca 25 m from the shoreline, at the point corresponding to the location of the nearshore wave gauge. The mean water depth at this location was 0.7–0.9 m (see Figure 10).
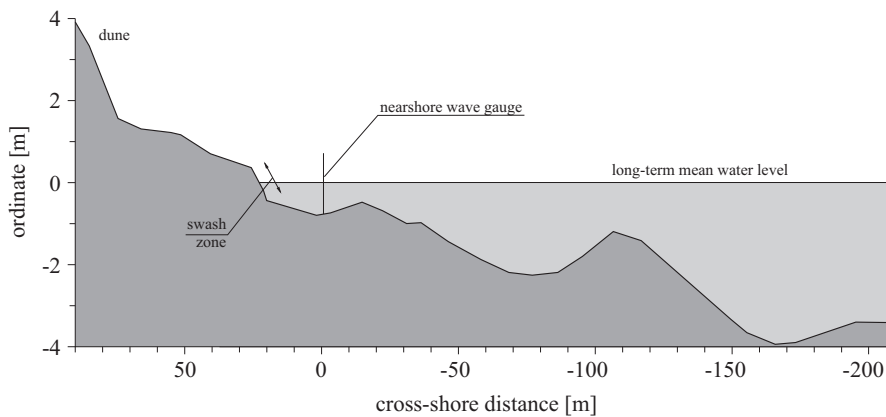
Figure 10. Nearshore seabed profile at CRS Lubiatowo

The data selected were taken during a 24 h period between 9 and 10 October 2006. The nearshore seabed profile was measured on these days at about 12:00 hrs. The bathymetric surveys were carried out using a geodesic rod and an electronic tachymeter, with a vertical accuracy of about 0.01 m. The irregular wave motion during the period under consideration was described by the representative wave parameters, i.e. the root-mean-square wave height $H_{rms} = 0.1$ m and the peak period $T_p = 7$ s. The run-up was recorded for 30 minutes at about 12:00 hrs on both 9 and 10 October 2006. During this 24 h period of measurements, the water level oscillated slightly between -1 cm below the long-term SWL and $+7$ cm above it.

Figure 11 shows a sequence of about 260 step-by-step run-up events (the extreme horizontal extent of a water tongue from some reference point) observed on 9 October 2006. The model results of wave run-up, together with the field data from 9 and 10 October are plotted in Figure 12. The thick line in the Figure indicates the range of the measured in situ wave run up, the dot is the mean run-up height based on measurements (the standard deviation is denoted here by the letter σ) and the cross shows the run-up height obtained from numerical computations.
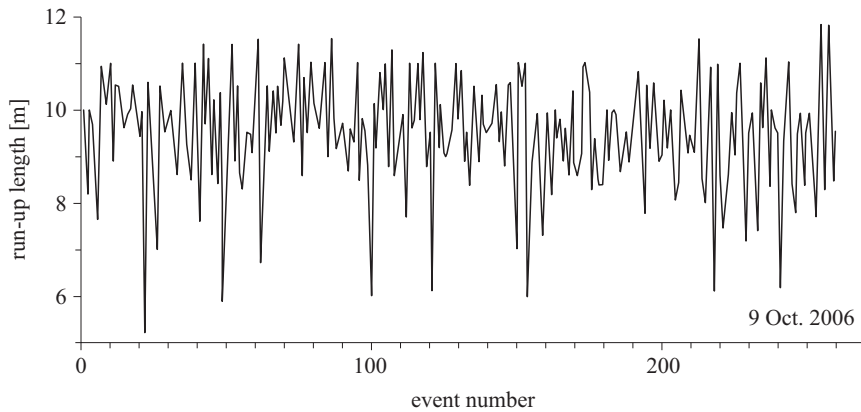
Figure 11. Run-up events registered during the 30 minutes of observations on 9 October 2006
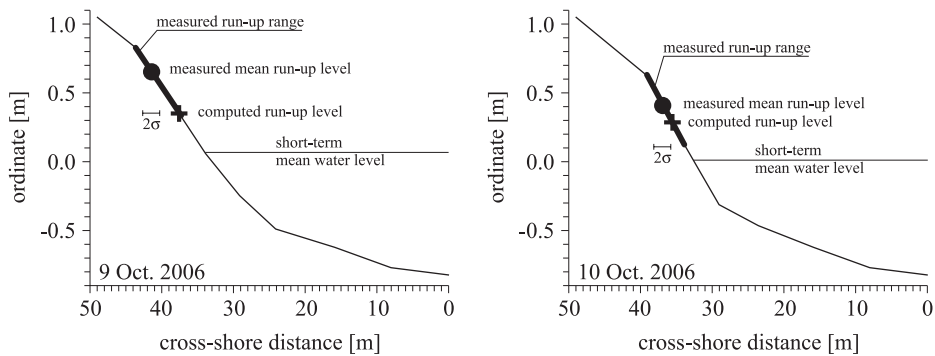
Figure 12. Wave run-up: model results vs. field data collected at CRS Lubiatowo on 9 and 10 October 2006

It can be seen in Figure 12 that the model run-up heights in both cases lie within the range of values measured in situ; nevertheless, these values are slightly underestimated, especially in the first case. Bearing in mind that the conditions actually recorded (random/irregular) are represented in

the model input by the representative wave parameters, namely the root-mean-square wave height H_{rms} and the peak period T_p, compliance can be regarded as satisfactory.

In the computations of sediment transport rates and the 24 h evolution of the beach face, the median grain size diameter was assumed to be $d_{50} = 0.22$ mm (with settling velocity $w_s = 0.028$ m s^{-1}), in accordance with the parameters of the actual sediment sampled in the nearshore zone of the Lubiatowo site. In the modelling of morphological bed changes, water level variations were taken into account. The results relating to the net sediment transport rates and the bottom changes are shown in Figures 13 and 14 respectively.
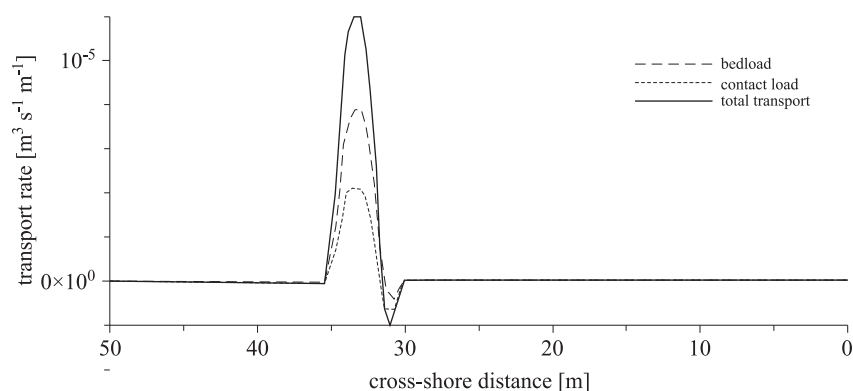
Figure 13. Computed sediment transport rates across the beach face at CRS Lubiatowo
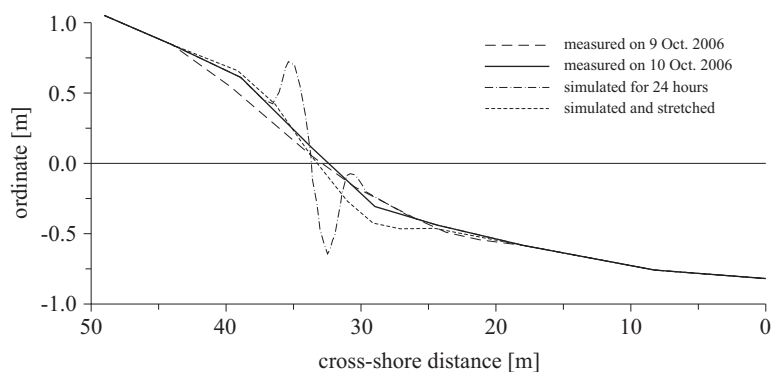
Figure 14. Beach face evolution (model results and field data) at CRS Lubiatowo on 9–10 October 2006

The computed net sediment transport rates shown in Figure 13 first decrease slightly and then increase rapidly in front of the intersection of the beach face with the still water level. Landwards of this intersection, the transport rates again decrease considerably.

Figure 14 presents the results of the 24 h numerical simulation of the nearshore sea bed changes (dashed-dotted line), together with the measured initial and final bottom profiles (dashed and solid lines respectively). The theoretical curve computed for the representative wave ($H_{rms} = 0.1$ m, $T_p = 7$ s) reflects features of the sediment transport rates from Figure 13. The significant spatial variability of the net transport rates concentrated around the shoreline point causes local significant erosion and accumulation effects. These effects correspond qualitatively to the observed beach face evolution.

The range of bottom changes caused by the representative wave spreads from 28.5 m to 37 m (see Figure 14). This is a much shorter distance than for measured random waves, for which changes were observed in the range 16 m–44 m. In order to take the above into account when comparing the model results with the measurements, the computed values (dashed-dotted line) were extended over the real area of sediment motion: the erosion and accumulation volumes were preserved. Thus, the original replacement of random wave trains by one representative regular wave was finally reconstructed by distributing the lithodynamic processes along the entire beach face affected by observed waves. The result of this transformation is also presented in Figure 14 (dotted line).

This extension of the computational results was necessary to convert the bottom profile evolution, theoretically caused by monochromatic hydrodynamic forcing, into the bottom changes resulting from the impact of actual random hydrodynamics. In its current version the model is incapable of dealing with irregular waves. The attempt to use the root-mean-square wave height and the wave peak period as input wave parameters is justified, however, since these quantities are representative of the energy of irregular waves and, consequently, of wave-induced bed shear stresses and sediment transport rates. Unfortunately, the assumed range of extension could not be estimated theoretically on the basis of any idea other than the measured limits of run-up on the beach face.

As can be seen in Figure 14, the modelled accumulation of sand in the run-up region agrees very well with the measured data, whereas the modelled erosion volume in the run-down area is distinctly overestimated. According to the model, the sediment volume conservation condition is satisfied on the cross-shore profile, causing the volumes of accumulation and erosion to be equal. Under natural conditions, this rule could be disturbed

by longshore sediment fluxes, even though the waves approached the shore almost perpendicularly in the case analysed here.

In general, the actual trend of beach face evolution, namely, that erosion in the run-down area is compensated by the run-up accumulation, is correctly represented in the model.

5. Concluding remarks

The paper discusses the application of a long wave run-up model to calculations of sediment transport rates and bottom changes in the swash zone. The results of numerical simulations for the theoretical case show that the model can produce reasonable results for standing waves on a plane slope.

For the purely theoretical case, the Lagrangian hydrodynamic model was thoroughly tested for the entire shallow-water region, with the focus on the swash zone. The tests revealed that the model is capable of simulating time-domain flow velocities and water surface elevations. The model reflects the variability in the hydrodynamic features along the swash zone and copes perfectly with the moving boundary problem related to the motion of the water tongue. The results of the lithodynamic component of the model indicate a tendency to carry the sediment from the run-down area landwards to the run-up area. As a consequence, the bottom slope in the swash zone becomes steeper.

The model yields correct results for waves with a relatively small steepness and for not too gentle slopes on the swashed part of the bottom; otherwise waves would break, and wave breakage is not represented in the hydrodynamic model.

The results for the theoretical case were used in an application of the modelling framework to the natural conditions of the sandy coast of the Baltic Sea. The relevant data were collected in 2006 at a non-tidal shore at the IBW PAN Coastal Research Station (CRS) at Lubiatowo (Poland). The agreement between the model run-up results and the measurements was found to be satisfactory. The simulated accumulation of sand in the landward part agrees very well with the measured data, but the erosion in the seaward part of the swash zone is distinctly overestimated. The latter may be due to some longshore current, even though the waves approached the shoreline almost perpendicularly. This implies that the model appears to be quite reliable in the context of wave run-up, but improvements will be needed to make it fully operational and useful for predicting wave-induced sediment transport in the swash zone.

The hydrodynamic model was developed within the Lagrangian framework. Therefore, the computations were carried out accurately from the

mathematical point of view without any approximations being made to the moving shoreline position. It should be pointed out, however, that the present modelling approach is applicable to a rather limited range of conditions, namely, non-breaking waves, which are seldom observed on natural beaches. Furthermore, the model does not simulate irregular sea waves and instead uses the representative wave parameters to reflect randomness. Finally, such phenomena as water infiltration into the sandy beach slope and the oblique approach of waves are not taken into consideration.

Despite the above limitations, the model results can shed some new light on the physical processes occurring in the swash zone. In view of the scarcity of experimental data on sediment transport during wave run-up, especially collected in actual field conditions, knowledge of swash zone lithodynamics is still insufficient and any progress in this area seems to be worthy of public presentation.

References

Alsina J. M., Baldock T. E., Hughes M. G., Weir F., Sierra J. P., 2005, *Sediment transport numerical modelling in the swash zone*, Proc. Coastal Dynamics '05, ASCE (CD), doi:10.1061/40855(214)105.

Baldock T. E., Alsina J. M., 2005, *On the transport of suspended sediment by a swash event on a plane beach*, Coast. Eng., 52 (9), 811–814, doi:10.1016/j.coastaleng.2005.06.003.

Butt T., Russell P., 2000, *Hydrodynamics and cross-shore sediment transport in the swash-zone of natural beaches: a review*, J. Coast. Res., 16 (2), 255–268.

Deigaard R., 1993, *Modelling of sheet flow: dispersion stresses vs. the diffusion concept*, Prog. Rep. 74, Inst. Hydrodyn. Hydraul. Eng., Tech. Univ. Denmark, 65–81.

Fredsøe J., 1984, *Turbulent boundary layer in combined wave-current motion*, J. Hydraul. Eng.-ASCE, 110 (HY8), 1103–1120, doi:10.1061/(ASCE)0733-9429(1984)110:8(1103).

Kaczmarek L. M., Ostrowski R., 1998, *Modelling of a three-layer sediment transport system in oscillatory flow*, Proc. 26th ICCE, ASCE, 2559–2572.

Kaczmarek L. M., Ostrowski R., 2002, *Modelling intensive near-bed sand transport under wave-current flow versus laboratory and field data*, Coast. Eng., 45 (1), 1–18, doi:10.1016/S0378-3839(01)00041-2.

Kapiński J., 2003, *Lagrangian-Eulerian approach to modelling of wave transformation and flow velocity in the swash zone and its Seaward vicinity*, Arch. Hydro-Eng. Environ. Mech., 50 (3), 165–192.

Kapiński J., 2006, *On modelling of long waves in the Lagrangian and Eulerian description*, Coast. Eng., 53 (9), 759–765, doi:10.1016/j.coastaleng.2006.03.009.

Kapiński J., Kołodko J., 1996, *Wave run-up on gentle slopes: a hybrid approach*, Arch. Hydro-Eng. Environ. Mech., 43 (1–4), 79–89.

Keller J. B., Keller H. B., 1964, *Water wave run-up on a beach*, Res. Rep. No. NONR-3828(00), Office Naval Res., Dept. Navy, New York.

Kobayashi N., 1999, *Wave runup and overtopping on beaches and coastal structures*, Adv. Coast. Ocean Eng., 5, 95–154.

Kobayashi N., Johnson B. D., 2001, *Sand suspension, storage, advection and settling in surf and swash zones*, J. Geophys. Res., 106 (C5), 9363–9376, doi:10.1029/2000JC000557.

Larson M., Kubota S., Erikson L., 2001, *A model of sediment transport and profile evolution in the swash zone*, Proc. Coastal Dynamics '01, ASCE, 908–917, 10.1061/40566(260)93.

Masselink G., Puleo J. A., 2006, *Swash zone morphodynamics*, Cont. Shelf Res., 26 (5), 661–680, doi:10.1016/j.csr.2006.01.015.

Nielsen P., 2002, *Shear stress and sediment transport calculations for swash zone modelling*, Coast. Eng., 45 (1), 53–60, doi:10.1016/S0378-3839(01)00036-9.

Ostrowski R., 2003, *A quasi phase-resolving model of net sand transport and short-term cross-shore profile evolution*, Oceanologia, 45 (2), 261–282.

Prasad R. S., Svendsen I. A., 2003, *Moving shoreline boundary condition for nearshore models*, Coast. Eng., 49 (4), 239–261, doi:10.1016/S0378-3839(03)00050-4.

Pritchard D., Hogg A. J., 2003, *On fine sediment transport by long waves in the swash zone of a plane beach*, J. Fluid Mech., 493, 255–275, doi:10.1017/S0022112003005901.

Pritchard D., Hogg A. J, 2005, *On the transport of suspended sediment by a swash event on a plane beach*, Coast. Eng., 52 (9), 1–23, doi:10.1016/j.coastaleng.2004.08.002.

Pruszak Z., Zawadzka E., 2005, *Vulnerability of Poland's coast to sea-level rise*, Coast. Eng. J., 47 (2–3), 131–155, doi:10.1142/S0578563405001197.

Shuto N., 1967, *Run-up of long waves on a sloping beach*, Coast. Eng. Japan, 10, 23–38.

Van Rijn L. C., Walstra D. J. R., Grasmeijer B., Sutherland J., Pan S., Sierra J. P., 2003, *The predictability of cross-shore bed evolution of sandy beaches at the time scale of storms and seasons using process-based profile models*, Coast. Eng., 47 (3), 295–327, doi:10.1016/S0378-3839(02)00120-5.

Zelt J. A., Raichlen F., 1990, *A Lagrangian model for wave-induced harbour oscillation*, J. Fluid Mech., 213, 203–225, doi:10.1017/S0022112090002294.